DESIGN OF BURNER PERFORMANCE OPTIMIZATION SYSTEM BASED ON LASER MACHINING

by

Banggui GUAN, Yanfu QIN, and Minglei GUO*

School of Electrical and Electronic Engineering, Anhui Science and Technology University, Bengbu, China

The existing burner performance optimization system neglects the measurement of single pulverized coal particle temperature in the combustion process, so the temperature control error is large, which leads to poor performance improvement of burner and poor control of residual oxygen. Therefore, a burner performance optimization system based on laser machining is designed. Design the overall frame of burner performance optimization. The performance optimization of the burner is mainly realized by the control of temperature and oxygen content. The gas quantity is calculated and fed back to the PID controller through the error value and the rate of temperature difference between the actual temperature and the set temperature. Based on the Hencken plane flame burner, an optical measuring system for single pulverized coal particle ignition based on laser processing is established to obtain the temperature of the particles. Based on this, the Proteus -based burner transient temperature distribution subsystem and the steady-state ANN model-based temperature control optimization algorithm are designed. The experimental results show that the burner of the system can control the residual oxygen very well, and the temperature control result of the system is highly fit with the simulation result, so the temperature control precision of the system is high.

Key words: *optical measurement system, residual oxygen control,*
burner performance optimization, laser processing,
temperature control

Introduction

The burner (Burner) is a general term for a device that allows the mixture of fuel and air to be fired in a certain manner and is essential in the heat-related industries of boilers, smelters, furnaces, heat treatment*, etc.* [1]. As the core of the whole heating device, it controls the power, temperature distribution, thermal efficiency and service life of the boiler and other controlled objects. Based on the burner, the technology of waste heat recovery is adopted to improve the thermal efficiency, energy saving and emission reduction of the combustion system by recovering the high heat gas. Therefore, the study of burner is of great significance under the new energy saving and emission reduction policy [2]. However, the burner is also faced with the performance and control optimization problems, especially the importance of solving these problems. Optimization of burner performance and control is a key technical problem that must be solved to promote the development of burner towards energy saving and emission reduction [3].

* Corresponding author, e-mail: bangguiguan@yeah.net

Dong *et al*. [4] proposes a hybrid optimization method based on quantum genetic algorithm and neural network. With the help of boiler combustion characteristic test data of power plant, the boiler combustion model of neural network is established, and the quantum genetic algorithm is used to optimize the secondary air door opening and burner swing angle of boiler combustion, so as to adjust the best set value of each optimization target, to realize the overall optimization and control of boiler combustion on thermal efficiency and nitrogen and oxygen emission. In Jia *et al.* [5], for the combustion process of biomass rotary burner, the non-adiabatic mixed fraction probability density function combustion model is adopted, and the effects of convective and radiant heat transfer losses are considered. The combustion process of biomass rotary burner is numerically simulated and analyzed by field synergy theory. The effects of the performance of biomass rotary burner and excess air coefficient on the combustion effect of biomass rotary burner were studied.

However, the aforementioned existing research methods ignore the temperature measurement of single pulverized coal particles in the combustion process, resulting in better control of burner temperature and residual oxygen. Therefore, a burner performance optimization system based on laser machining is designed.

Burner performance optimization system based on laser machining

Overall framework of burner performance optimization

The overall design goal of burner performance optimization is to lay a foundation for the future study of burner performance optimization by determining the overall framework with clear ideas [6]. Figure 1 is a schematic diagram of the overall framework for burner performance optimization.
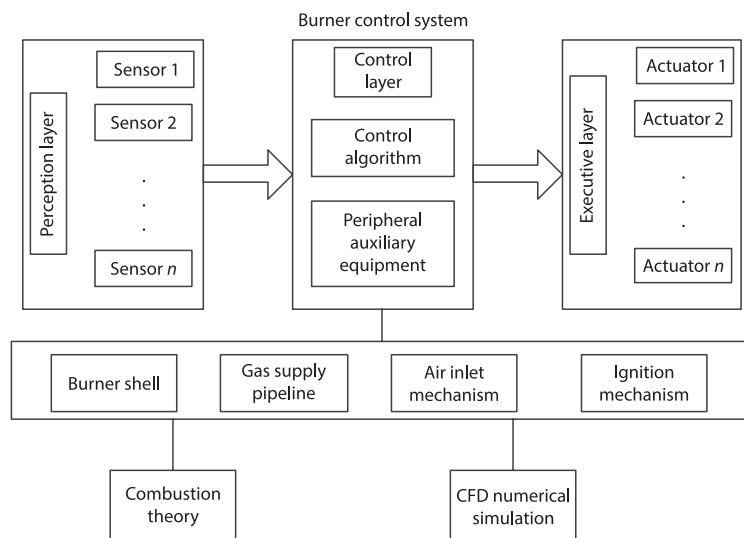

Figure 1. Overall framework of burner performance optimization

As can be seen from fig. 1, the burner is composed of two parts: the body structure and the control system. The body structure includes the parts such as the shell of the burner, fuel pipe-line, air pipe-line, ignition mechanism, valve group mechanism*, etc.* These parts have been briefly described in the first chapter of the burner overview, and the previous design is based on the combustion theory [7]. The control system consists of three layers, *i.e.*, perceptual

layer, control layer and executive layer. The former layer is responsible for data perception and acquisition, and sends the collected data to the control layer to provide the basis for real-time control guidance. The latter layer directly executes the burner combustion timing and optimal combustion, and the control object includes various valve switches. The control layer is the core of the optimized control framework and is responsible for scheduling and controlling the whole combustion task.

Design of residual oxygen control structure and program

The overall structure of the residual oxygen control system of the burner combustion system can be divided into residual oxygen measurement, fuzzy neural network controller, fuzzy controller, air valve, gas valve*, etc.* the specific structure is shown in fig. 2.
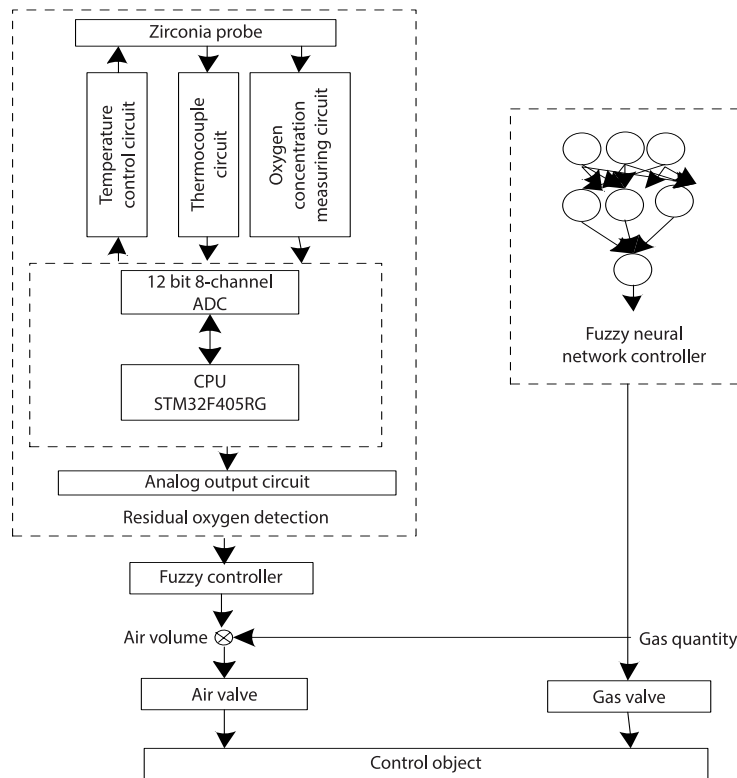
Figure 2. Structure diagram of residual oxygen control system

According to fig. 2, the system can be divided into residual oxygen control part and residual oxygen measurement part. The specific description is:

– The residual oxygen control part is mainly composed of a fuzzy neural network controller and a fuzzy controller, the former being an input layer with two nodes, representing the temperature error value of the burner and the rate of temperature difference change. The latter being an output layer with one node, representing the gas quantity [8, 9]. The fuzzy neural network controller calculates the gas quantity feedback to the PID controller through the error value between the actual temperature of the burner and the setting temperature and the rate of temperature difference. In order to satisfy the actual value of gas quantity, PID controller uses gas valve to adjust the gas quantity.

– The residual oxygen measurement part includes oxygen concentration detection and oxygen concentration 4~20 mA output circuit, temperature control circuit and human-computer interaction module.

The residual oxygen is measured by a zirconia sensor. At mV level, the analog quantity representing oxygen content is prone to electromagnetic interference. In order to avoid this phenomenon, the valuable analog signal needs to be enlarged before entering the filter circuit. Use AD to select high quality signal, transfer to IC protocol, finally reach the master chip, complete data management. Since the zirconia sensor can operate only when the furnace temperature reaches 720 °C, the temperature module is set, which is responsible for providing the burner temperature data to the MCU. The PID controller controls the temperature of continuous burner according to the temperature data processed by SCM to ensure the operating temperature of zirconia sensor. Select HMI serial screen to realize man-machine interaction with serial port and master chip. The HMI display receives the command from the main control circuit to display the temperature value and residual oxygen concentration value. When the temperature cannot meet the requirements of zirconia operation, the staff uses the screen to reset PID parameters to control the heating power, so that the continuous burner is raised to the operating temperature of the zirconia sensor.
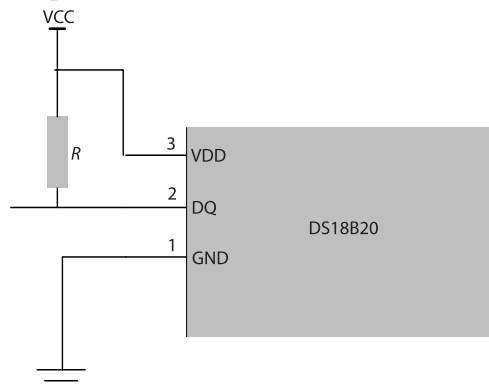

Figure 3. Temperature acquisition circuit

Temperature data acquisition is very important in the residual oxygen control system of burner combustion system. The single bus of thermocouple circuit is selected to transfer temperature data and a certain end of I/O port is used to realize signal transmission [10]. Analog temperature transmission and data signal management are carried out through DS18B20, in which AT89S52 is used to sort out the data and determine the temperature collection range to complete the temperature collection task. The specific circuit is shown in fig. 3.

According to fig. 3, the temperature data is collected by DS18B20 and transmitted to port AT89S52, or P3.3, which is the signal input of the system. The DS18B20 and AT89S52 co-operate with each other to complete the task of temperature acquisition, the system temperature acquisition circuit structure is simple, so the wider scope of application.

When the electrical reset, the system measurement program to start. The main controller ARM is responsible for regulating the heating power of the heater, so that the furnace temperature can meet the operation requirements of zirconia probe. Therefore, the program needs to continuously measure the furnace temperature and display the temperature of the zirconia probe to the display screen at any time. If the temperature is not up to 720 °C, the data collected by the main controller of the PID algorithm to obtain 4-20 mA signal to heat the heater [11, 12]. If the temperature can make the zirconia probe run, the residual oxygen collection program starts. Through the processing of oxygen potential signal, the specific value can be read on the display screen, and the obtained oxygen potential information needs to be converted into 4-20 mA current signal and fed back to the controller. When all the programs are finished, start the next cycle. Figure 4 shows the flow of the measurement program.

According to fig. 4, the measurement process from start to the output, after the port is initialized, the system default, load parameters, such as, running, sampling temperature, tem-

perature control, electric potential, data processing, including setting parameters, storage, temperature overheat alarm and accidentally break protection, PC, according to the modules of the burner combustion system residual oxygen control system of residual oxygen measurement process.

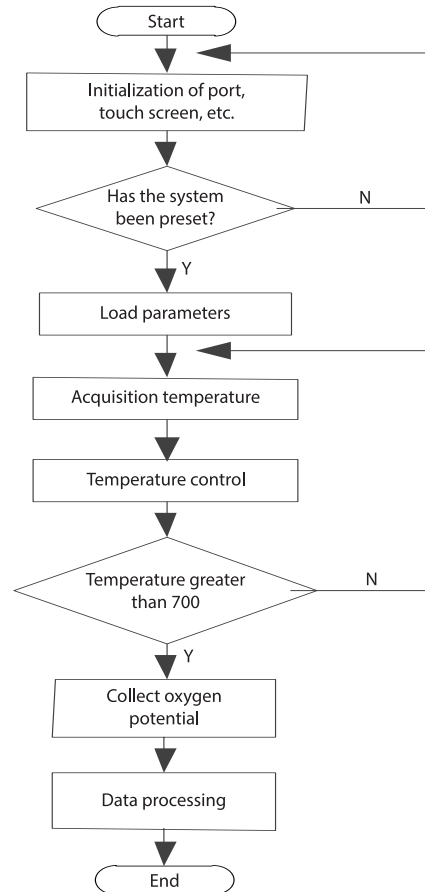*Optical measurement structure of single pulverized coal based on laser processing*

Optical measurement system for single pulverized coal particle ignition based on Hencken flat flame burner core, as shown in fig. 1. The burner is mainly divided into three layers: a mixture of CO and H_2 fuel gas through more than 400 capillary tubes with an internal diameter of 0.6 mm into the furnace, a mixture of N_2 and O_2 oxidized gas through honeycomb rectifier mixed with fuel gas on the surface of the burner, and in addition, the burner's outermost outer layer is also provided with an outer ring gas passage, through the input of N_2 to protect the flow field and cool the burner [13, 14]. The center of the burner is provided with a powder feeding pipe with an inner diameter of 2 mm, which is fed into the N_2 and carries coal powder into the furnace. After passing through the plane flame, the cold pulverized coal particles are heated rapidly at a heating rate of 105-106 K/s. A transparent quartz square tube with the size of 54 mm × 54 mm is arranged above the burner as the furnace chamber of the burner, which not only ensures the stability of the flow field above the burner, but also creates a good environment for the ignition combustion of coal particles and optical measurement.

Figure 4. Measurement flow chart of residual oxygen control system

The two-color method is used to measure the temperature of single particle of coal powder. Since the ignition temperature of pulverized coal particles is below 3000 K, the Wien equation is used to replace the Planck radiation equation, and the error is negligible:

$$I(\lambda, T) = \varepsilon(\lambda) \frac{C_1}{\lambda^5} e^{C_2/\lambda T} \qquad (1)$$

where λ is the wavelength corresponding to the radiation intensity, T – the temperature corresponding to the radiation intensity, $\varepsilon(\lambda)$ – the emissivity of pulverized coal, and C_1 and C_2 are empirical parameters. By comparing the light radiation intensity of the same object at two wavelengths at the same position, the temperature of the object can be obtained:

$$T = \frac{C_2 \left(\dfrac{1}{\lambda_2} - \dfrac{1}{\lambda_1} \right)}{\ln \dfrac{I(\lambda_1, T)}{I(\lambda_2, T)} - \ln \dfrac{\varepsilon(\lambda_1, T)}{\varepsilon(\lambda_2, T)} - \ln \dfrac{\lambda_2}{\lambda_1}} \qquad (2)$$

The data values received by the high speed camera are related to the optical path characteristics and the photographed object. For a single CMOS photosensitive unit, the total radiation intensity received is the integral of the incident light intensity to the wavelength and time. This paper simplifies it here. The camera output data R, G, and b values at a specific exposure time are 700 nm wavelength radiation intensity $IR(\lambda, T)$, 546 nm wavelength radiation intensity $IG(\lambda, T)$. As a function of 435 nm wavelength radiation intensity $IB(\lambda, T)$, the relationship between output RGB data and radiation intensity is determined through blackbody furnace calibration [15]. In the actual ignition image of pulverized coal particles, because the signal-to-noise ratio of B value is low, the ratio of R and g value is selected. Here, the ash body assumption is made for pulverized coal particles to obtain the calculation equation of temperature:

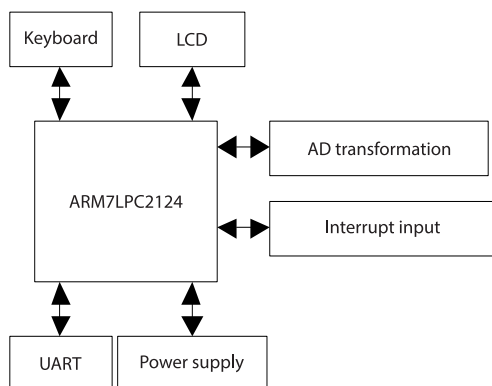$$T = \frac{C_2\left(\dfrac{1}{\lambda_2} - \dfrac{1}{\lambda_R}\right)}{\ln\dfrac{R\lambda_G}{GK}} \tag{3}$$

Through the calibration of blackbody furnace, the corresponding curves of R, G, B and $IR(\lambda, T)$, $IG(\lambda, T)$ and $IB(\lambda, T)$ can be established, in which D is the response proportion coefficient, which can be brought into the equation to calculate the particle temperature

Transient temperature distribution subsystem of burner based on proteus

Proteus software not only has other EDA software experimental simulation function, but also can simulate SCM and peripheral devices, is the world's most reliable simulationols. Proteus software can realize schematic construction, code debugging to embedded chip and peripheral circuit simulation, also can switch to the wiring design module with one key, can truly achieve the integration design of concept to shape. Proteus software processor model supports a variety of translators, but also support 8051, ARM and so on.

Proteus software not only has a series of functions such as schematic lay-out, PCB and custom wiring, but also has two revolutionary advantages, one is interactive circuit simulation, the other is to simulate the processor and its peripheral circuit [16].

After designing and drawing the schematic diagram in Proteus software, it loads the compiled object code file and starts to run. It can observe the operation of the circuit in Proteus schematic diagram.

The core chip of ARM7TMDI is selected as the hardware chip of the burner transient temperature field simulation system, considering the function, power consumption and cost of the system. Considering the wide application, LPC2124 is chosen as the hardware platform.

The LPC2124 is a 32-bit single-chip ARM microcontroller, which is based on an embedded chip supporting real-time online analog simulation and simultaneous tracking. It has 256 KB memory and 128-bit memory interface. Can strictly control the size of source code, code size effectively reduced. Figure 5 shows the overall hardware architecture.

Figure 5. Overall hardware architecture

Guan, B., *et al.*: Design of Burner Performance Optimization System Based ...
THERMAL SCIENCE: Year 2022, Vol. 26, No. 3A, pp. 2397-2408

2403

The system is mainly for the experimental simulation of burner transient temperature field distribution. The design goal is to use PROTEUS software to design the experimental model, so as to understand the overall distribution of burner temperature field. Considering the actual needs, the hardware circuit is divided into display module, keyboard module, digital to analog conversion module, interrupt module, bus communication module, serial communication module and so on, fig. 6.

(a)   (b)
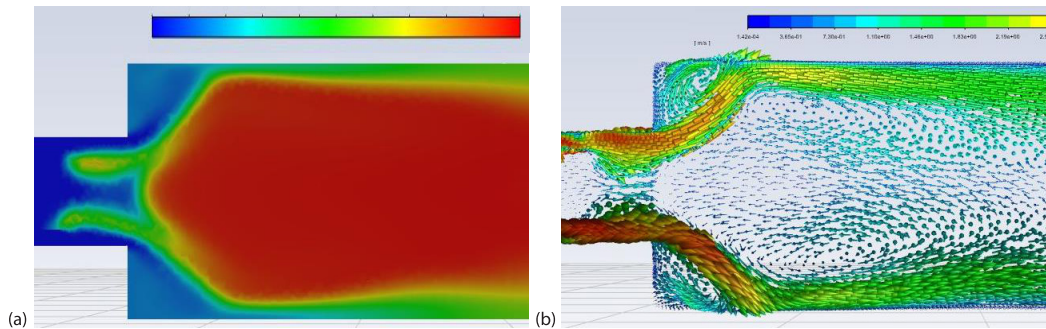
Figure 6. Proteus simulation results (a) simulation results of heat flow and (b) simulation results of temperature distribution

Steady-state ANN model

The steady-state ANN is described:

Step 1. After determining the structure of the artificial neural network, the number of points in the input layer and the number of nodes in the hidden layer, and completing the initial setting of the weight coefficient of each layer, the appropriate learning rate and inertia factor shall be selected.

Step 2. Calculating the input and output of each layer of the ANN, and taking the adjustable parameters h_p, h_i, and h_dQ of the controller as the final output of the network.

Step 3. Select the incremental digital PID control algorithm to realize the calculation of the controller output.

Step 4. Implement network learning and complete the online adjustment of weight coefficient, and adjust PID control parameters adaptively.

Step 5. Return *Step 2*.

The input of the ANN:

$$X_j = x(j), \quad j = 1, 2, 3 \tag{4}$$

where x is the input parameter.

The inputs and outputs of the hidden layer of the ANN:

$$X_i(h) = f_i\left[\left(h_p\right)\right], \; i = 1, 2, ..., T \tag{5}$$

$$Y_i(h) = \sum_{j=0} \Re_{ij}^{(2)} X_j^{(1)} \tag{6}$$

where the weight coefficient of hidden layer is $\Re_{ij}^{(2)}$, f_1 and T are the activation function of hidden layer neurons and the number of hidden layer nodes, respectively.

The sigmoid function:

$$f_1(x) = \frac{1}{1+e^{-x}} \tag{7}$$

The inputs and outpuf the output layer of the ANN:

$$net_l(h) = \sum_{i=0}^{H} \Re_{li}^{(3)} X_i^{(2)}(h) \tag{8}$$

$$Q_l(h) = f_2 \left[net_l^{(3)}(h) \right], \ l = 1, 2, 3 \tag{9}$$

where l is the number of output nodes and f_2 – the activation function of neurons in the output layer. Since the output is three adjustable parameters of PID, l takes values of 1, 2, and 3.

The output range is increased by a linear function:

$$f_2(x) = net_l^{(3)}(h) + Q_l^{(3)}(h) \tag{10}$$

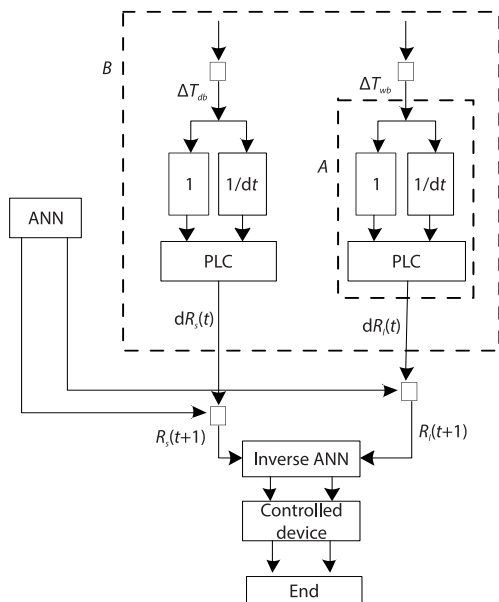## Optimization algorithm of temperature control based on steady-state ANN model

Based on the steady-state ANN model control principal control algorithm, the whole temperature control process is divided into A and B processes.

Process A obtains the error signal by comparing the combustion flow quantity and water content with the set value, then inputs the error signal into the fuzzy logic controller (FLC) for processing, and calculates the change value of the intermediate control variable as the adjustment value of the wall temperature. Process B is composed of ANN and inverse ANN model, which is mainly based on the required combustion temperature to calculate the required damper opening and hot air damper opening, combined with A process to complete the combustion process temperature control.

In the control process B, firstly, the output temperature corresponding to the current required exhaust damper opening and hot air damper opening of the burner is calculated by the steady-state ANN model. The target output of the burner at the next time is the sum of intermediate control variables calculated by $R_s(t)$, $R_l(t)$ and FLC of the current burner, which are $R_s(t + 1)$ and $R_l(t + 1)$, respectively.

Then, through the inverse ANN model, the calculated tide exhaust damper opening and hot air damper opening corresponding to $R_s(t + 1)$ and $R_l(t + 1)$ are transmitted to the controlled device as the actual control signal to complete the whole process temperature control of the burner, see fig. 7 for details.

Figure 7. Temperature control principle based on steady-state ANN model

Guan, B., *et al.*: Design of Burner Performance Optimization System Based ...
THERMAL SCIENCE: Year 2022, Vol. 26, No. 3A, pp. 2397-2408

2405

Experimental design and result analysis

Simulation test was carried out in a fuel burning power plant. The fuel burner equipped in the plant is 2×400 tonne per day, the average annual fuel handling capacity is 292000 tonnes, and the condensing turbo-generator set of 1×15 MW is used for operation, and the full-load evaporation capacity of the unit is 39 tonne per hour. Burner row for a domestic manufacturers complete set of supply. At present, the auxiliary combustion air distribution in the plant mainly relies on manual work, and the performance optimization method of the burner is applied.
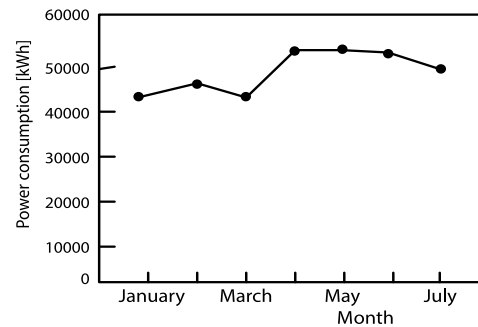
Comparison of power consumption before and after burner performance improvement

Firstly, the energy consumption before and after delivery is compared. The comparison of power consumption before and after the application of the proposed method is shown in tab. 1 and fig. 8.

Table 1. power consumption records before and after burner transformation

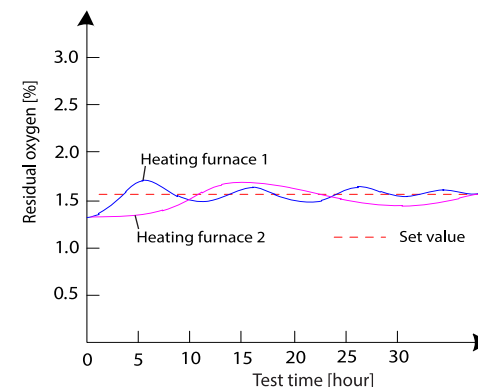| Running period	Running time [day]	Power consumption [kWh]	Annual power consumption [kWh]	Annual energy saving [kWh]
Before transformation	280	210632	1546256	82460
After transformation	280	94100	792000	

By using this method, not only the adjustment speed of air pressure and flow rate is fast and the adjustment precision is high, but also the service life of the fuel burner is improved, and the stable operation is ensured. Since put into use in January, energy-saving economy effect is remarkable. By applying the proposed method to the fuel burning power plant, the dynamic response speed of fan outlet and the accuracy of air-flow control are improved, the labor of operators is reduced, the utilization ratio of the burner is improved and the equipment is operated stably.

Figure 8. Comparison of power consumption before and after burner performance improvement

Residual oxygen control effect of burner

In this paper, the system controls the residual oxygen of the burner combustion system through the fuzzy controller. In order to test the effect of the fuzzy controller of this system, the control data of residual oxygen of No. 1 burner and No. 2 burner are obtained experimentally and compared and analyzed. The specific results are shown in fig. 9.

As can be seen in fig. 9, the Burner 1 combustion system in this system can be used to control the amount of residual oxygen for a short period of time and can be adjusted as quickly as

Figure 9. Comparison of residual oxygen control of No. 1 and No. 2 burners

2406

Guan, B., *et al*.: Design of Burner Performance Optimization System Based ...
THERMAL SCIENCE: Year 2022, Vol. 26, No. 3A, pp. 2397-2408

possible according to the set value. On the contrary, the control performance of No. 2 burner is obviously inferior to No. 1. When the residual oxygen quantity fluctuates greatly, it cannot be controlled in time and the required value can be restored. Therefore, this system can control the residual oxygen more quickly and stably.

During the working period of the two burners in July 2021, two days of the burners shall be randomly selected to measure the residual oxygen of the burners. Under the continuous working conditions of the Burners No. 1 and No. 2, the residual oxygen data displayed on the touch screen shall be recorded for two hours, and the average residual oxygen value of the flue gas at No. 1 and No. 2 shall be compared, and the average value of the Burner No. 2 shall be subtracted by the average value of the Burner No. 1 to obtain the drop value of residual oxygen. In the experiment, the residual oxygen value of the two burners shall be selected to ensure the universality of the verification effect. The specific measurement value is shown in tab. 2.

Table 2 Data value of residual oxygen of Burner 1 and 2

Date	Time	Burner 1 [%]	Burner 2 [%]
July 10th	8 a. m.	0.3	1.9
	10 a. m.	1.2	3.8
	12 a. m.	2.6	2.8
	2 p. m.	0.5	1.8
	4 p. m.	2.1	3.5
	Average	1.34	2.76
July 11th	8 a. m.	1.5	1.5
	10 a. m.	0.5	4.8
	12 a. m.	1.2	3.6
	2 p. m.	1.1	1.8
	4 p. m.	1.5	2.5
	Average	1.16	2.84

According to the residual oxygen data measured in tab. 2, the average residual oxygen values of Burner 1 on July 10 and 11 are 1.34% and 1.16%, respectively, and the average residual oxygen values of Burner 2 on July 10 and 11 are 2.76% and 2.84%, respectively. Therefore, the Burner No. 1 of this system can well control the residual oxygen.
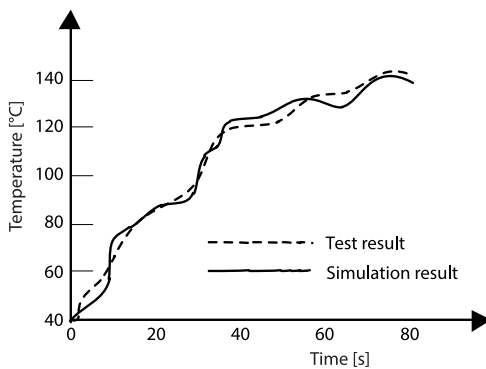
Figure 10. Test results and simulation results under rated conditions

Burner temperature simulation test

Burner rated state test: in this case, the burner temperature simulation is carried out, and a temperature value is selected at an interval of 20 seconds. Based on the burner temperature test data and simulation data, the temperature change curve under time change is shown in fig. 10.

Analysis of fig. 10 shows that there is some error between the temperature test data and the simulation data of the burner at the same time. The reason for the error is that the burner is simplified in the process of modelling, and the

Guan, B., *et al.*: Design of Burner Performance Optimization System Based ...
THERMAL SCIENCE: Year 2022, Vol. 26, No. 3A, pp. 2397-2408

2407

heat dissipation effect of the burner is poor in the actual temperature test, which directly affects the actual test results. As a whole, the variation of temperature is approximately the same, which indicates that the experimental simulation system based on Proteus has good operation effect and high precision.

Burner peak temperature test: 5 seconds choose a temperature value, get burner test temperature data, based on burner temperature test data and simulation data, get the time change temperature curve as fig. 11.

It can be seen from the analysis of fig. 11 that the fitting between the test results and the simulation results under the peak condition is higher, which shows that the accuracy of the system test results is strong.
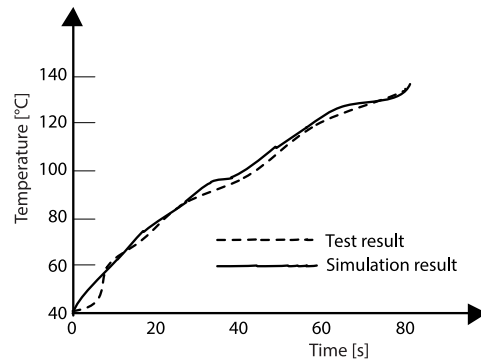
Figure 11. Test results and simulation results under peak conditions

Conclusions

A burner performance optimization system based on laser machining is designed. The overall frame of burner performance optimization is designed to complete the scheduling control of combustion tasks. The performance optimization of the burner is mainly realized by the control of temperature and oxygen content. Through the design of residual oxygen measurement, fuzzy neural network controller, fuzzy controller, air valve and gas valve, the residual oxygen control is realized. Fuzzy neural network controller is introduced to calculate the gas quantity feedback to PID controller through the error value and temperature change rate between the actual temperature and the set temperature. Design the temperature collection circuit and residual oxygen flow, the temperature data are collected and transmitted to AT89S52 port by DS18B20. Based on the Hencken plane flame burner, an optical measuring system for single pulverized coal particle ignition based on laser processing is established to obtain the temperature of the particles. Based on this, the Proteus -based burner transient temperature distribution subsystem and the steady-state ANN model-based temperature control optimization algorithm are designed.

In order to verify the performance improvement effect of the designed system, a simulation experiment is designed. The experimental results show that the burner's power consumption is obviously reduced before and after the performance improvement, and the burner can control the residual oxygen and temperature very well.

Acknowledgment

Reference

[1] Smith, D. J., Simpson, K., Burner Control Assessment (Example) – Science Direct, The Safety Critical Systems Handbook, *5* (2020), pp. 217-230
[2] Hidegh, G., *et al.*,Distributed Combustion of Diesel-Butanol Fuel Blends in a Mixture Temperature-Controlled Burner, *Fuel*, 307 (2020), 121840

[3]   Bulysova, L. A., *et al.*, The GT-16 Gas Turbine Low-Emission Combustor, Results of Tests in a Single-Burner Chamber on the Stagnation Property Test Facility. Power Technology and Engineering, *54* (2021), 5, pp. 695-698

[4]   Dong, H. S., *et al.*, Boiler Combustion Optimization Control Based on Quantum Genetic Algorithm and Neural Network (in Chinese), *Machinery Design & Manufacture*, *4* (2020), 11

[5]   Jia, G. H., *et al.*, Field Synergy Analysis of Combustion Process of Biomass Rotary Burner (in Chinese), *Journal of Central South University*, *Science and Technology*, *52* (2021), 1, 8

[6]   Singh, A., *et al.*, Control Implementation of Squirrel Cage Induction Generator Based Wind Energy Conversion System, *Journal of Scientific and Industrial Research*, *79* (2020), 4, pp. 306-311

[7]   Jozsa, V., Mixture Temperature-Controlled Combustion, a Revolutionary Concept for Ultra-Low NOx Emission, *Fuel*, *291* (2021), 120200

[8]   Lee, C., *et al.*, Experimental Investigation of Air-Fuel Mixing Effects on Flame Characteristics in a Direct Fired Burner, *Energie*s, *14* (2021), 12, 3552

[9]   Ma, P., *et al.*, Effects of Na and Fe on the Formation of Coal-Derived Soot in a Two-Stage Flat-Flame Burner, *Fuel*, *265* (2020) II, 116914

[10] Dors, O. L., *et al.*, Chemical Abundances of Seyfert 2 AGN – I. Comparing Oxygen Abundances from Distinct Methods Using SDSS, *Monthly Notices of the Royal Astronomical Society*, *492* (2020), 1, pp. 468-479

[11] Shafaghatian, N., *et al.*, Damping Controller Design Based on FO-PID-EMA in VSC HVDC System to Improve Stability of Hybrid Power System, *Journal of Central South University*, *27* (2020), 2, pp. 403-417

[12] Tashan, T., *et al.*, Design and FPGA Implementation of Immune-PID Controller Based on BBO Algorithm for Heart Rate Regulation, *International Journal of Intelligent Engineering and Systems*, *14* (2021), 2, pp. 432-440

[13] Si, M., *et al.*, Study on the Combustion Behavior and Soot Formation of Single Coal ParticleUsing Hyperspectral Imaging Technique, *Combustion and Flame*, *233* (2021), 111568

[14] Butakov, E. B., *et al.*, Ignition Test for Mechanically Activated Pulverized Coal in a Vertical Tubular Reactor, *Thermophysics and Aeromechanics*, *27* (2020), 1, pp. 145-152

[15] Sosin, D. V., *et al.*, Increasing the Efficiency and Increasing the Resource of the Plasma-Ignition System by Its Modernization at Gusinoozerskaya TPP, *Thermal Engineering*, *68* (2021), 4, pp. 302-309

[16] Zhang, J., *et al.*, Study on Combustion Characteristics and NOx Emission of Low Swirl Combustor (in Chinese), *Computer Simulation*, *37* (2020), 7, pp. 260-265